Physical performance level in sarcomeric mitochondria creatine kinase knockout mouse model throughout ageing

R. Niel, L. Le Moyec, T. Launay, L. Mille-Hamard, M.N. Triba, Olek Maciejak, V.L. Billat, I. Momken

Physical performance level in sarcomeric mitochondria creatine kinase knockout mouse model throughout ageing

Niel R[1], Le Moyec L[1,2], Launay T[3], Mille- Hamard L[1], Triba MN[4], Maciejak O[5], Billat V[1], Momken I[1,6]

1. Université Paris-Saclay, Université d'Evry, 23 Boulevard François Mitterrand, 91000 Évry-Courcouronnes, France
2. Unité Molécules de Communication et Adaptation des Micro-organismes (MCAM) UMR7245 CNRS/Muséum National d'Histoire Naturelle, 63, rue Buffon CP54 75005 Paris, France
3. Université de Paris, Animal Genetic and Integrative Biology, INRAE, University of Paris-Saclay, AgroParisTech, 78350, Jouy-en-Josas, France
4. Université Paris 13, Sorbonne Paris Cité, Laboratoire Chimie, Structures, Propriétés de Biomatériaux et d'Agents Thérapeutiques (CSPBAT), Unité Mixte de Recherche (UMR) 7244, Centre National de Recherche Scientifique (CNRS), France
5. Unité d'Analyse et Modélisation pour la Biologie et l'Environnement (LAMBE), Université Paris-Saclay, Univ Evry, Evry, France
6. Université Paris-Saclay, Faculté de Pharmacie, Inserm, UMR-S 1180, Châtenay-Malabry, France

Corresponding author

Iman Momken

Email: Iman.momken@universite-paris-saclay.fr

Key words: *ageing; exercise performance; mitochondrial creatine kinase; skeletal muscle; efficiency*

Abstract

Purpose: The objective of the present study was to establish the role of sarcomeric mitochondrial creatine kinase (Mt-CK) in muscle energy output during exercise in a murine model of ageing (the Mt-CK knock-out mouse, Mt-CK $^{-/-}$).

Methods: Three age groups of Mt-CK$^{-/-}$ mice and control male mice (6, 9, and 18 months of age) underwent incremental treadmill running tests. The maximum speed (Vpeak) and maximal oxygen consumption (VO_2peak) values were recorded. Urine samples were analyzed using metabolomic techniques. The skeletal muscle (quadriceps) expression of proteins involved in mitochondria biogenesis, peroxisome proliferator-activated receptor gamma coactivator 1-alpha (PGC-1α) and dynamin-related GTPase mitofusin 2 (Mnf2) were quantified.

Results: The VO_2 peak (normalized to heart weight: HW) of 18-month-old (mo) Mt-CK $^{-/-}$ mice was 27% ($p<0.001$) lower than in 18-mo control mice. The VO_2peak /HW ratio was 29% ($p<0.001$) lower in 18-mo Mt-CK $^{-/-}$ mice than in 6-mo ($p<0.001$) and 32% ($p<0.001$) than 9-mo Mt-CK $^{-/-}$ mice. With a 0° slope, Vpeak was 10% ($p<0.05$) lower in 18-mo Mt-CK $^{-/-}$ mice than in 6-mo Mt-CK $^{-/-}$ mice but did not differ when comparing the 18-mo and 6-mo control groups. The skeletal muscles weight normalized on body weight in 6-mo Mt-CK $^{-/-}$ were 13 to 14% ($p< 0.001$, $p<0.05$) lower versus the 6-mo control, in addition, the presence of branched-chain amino acids in the urine of 6-mo Mt-CK $^{-/-}$ mice suggests an imbalance in protein turnover (catabolism rather than anabolism) but we did not observe any age-related differences. The expression of PGC-1α and Mnf2 proteins in the quadriceps showed that age-related effects were more prominent than genotype effects.

Conclusion: The present study showed ageing is potentialized by Mt-CK deficiency with regard to VO_2peak, Vpeak and mitochondrial protein expression. Our results support that Mt-CK$^{-/-}$ mice undergo physiological adaptations, enabling them to survive and to perform as well as wild-type

mice. Furthermore, it is possible that these adaptations in Mt-CK$^{-/-}$ mice have a high energy cost and might trigger premature ageing.

Abbreviations:

AK: Adenylate Kinase

BCAAs: Branched-chain amino acids

BW: Body Weight

CK: Creatine kinase

CK$^{-/-}$: Cytosolic creatine kinase, Mitochondrial creatine kinase knock out

Cr: Creatine

CS: Citrate synthase

Drp-1: Dynamin-related protein 1

EDL: Extensor digitorum longus

HW: Heart Weight

KO: Knock-out

MM-CK: Cytosolic creatine kinase

MM-CK$^{-/-}$: Cytosolic creatine kinase knock out

Mt-CK: Mitochondrial creatine kinase

Mt-CK$^{-/-}$: Mitochondrial creatine kinase knock out

Mfn2: mitochondrial membrane fusion factors dynamin-related GTPase mitofusin 2

mo: Month

OPLS: Orthogonal projection on latent structure

Opa1: Optic atrophy protein 1

PCr: Phosphocreatine

PGC-1α: Peroxisome proliferator-activated receptor gamma coactivator 1-alpha

TA: Tibialis

VO_2: Oxygen uptake

VO_2peak: Maximal oxygen uptake

Vpeak: Maximal speed

1. Introduction

Of the various mechanisms that contribute to metabolic homeostasis, energy transfer pathways have important roles in reacting rapidly to changes in energy requirements and the intensity of physical activity. In skeletal muscles and the heart, creatine kinase (CK) is required during rapid energy transitions. A decrease in gene expression and enzymatic activity of the sarcomeric mitochondrial creatine kinase (Mt-CK) and the cytosolic isoform (MM-CK) has been observed in senescent skeletal or cardiac muscles in both humans and rodents (Bodyak et al. 2002; Kaczor et al. 2006; Nemutlu et al. 2015; Nuss et al. 2009; Tepp et al. 2016). This decline in CK activity might be caused by oxidative stress (Nuss et al. 2009) and is one of the key factors in the loss of muscle function with age (Kaczor et al. 2006; Nuss et al. 2009; Pastoris et al. 2000).

The phosphocreatine/creatine (PCr/Cr) shuttle contributes significantly to energy transfer by regenerating PCr and increasing the availability of ADP for mitochondrial respiration (Miotto and Holloway 2016; Tepp et al. 2016; Ydfors et al. 2016). The PCr and Cr diffuse around 2000 times faster than ADP and ATP through the mitochondrial outer membrane and the cytosol (Kaldis et al. 1997), which allows efficient energy transfer - especially during intense physical activity.

Among the different isoforms of CK, the sarcomeric Mt-CK is bound to the outer surface of the inner mitochondrial membrane, so that the ATP generated by oxidative phosphorylation can be transphosphorylated to PCr. The Mt-CK forms a complex with voltage-dependent anion channels and adenine nucleotide translocase within the mitochondria membrane (Schlattner et al. 2001; Schlattner et al. 1998)

Creatine kinase knock-out mouse models Mt-CK$^{-/-}$, MM-CK$^{-/-}$ or both CK$^{-/-}$ were created by Wieringa's research group (Steeghs et al. 1998). This targeted mutagenesis made it possible to study respective roles of the two isoforms in exercise adaptations in these mice (Momken et

al. 2005; van Deursen et al. 1993; Veksler et al. 1995). A few studies proposed that $CK^{-/-}$ mice have alternative mechanisms or cytoarchitectural rearrangements for maintaining efficient energy transfer and signal transduction between ATP synthesis sites and ATPases (Kaasik et al. 2003; Novotova et al. 2006; Wallimann 2015). The muscles and hearts of MM-$CK^{-/-}$ mice have normal levels of PCr, ATP, and Cr because of the presence of Mt-CK in the interspace of mitochondria membranes. However, the limb muscles are unable to contract efficiently at the beginning of a stimulation period, and an electron microscopy analysis has shown a greater number of mitochondria and a higher mitochondrial volume in skeletal muscle fast-twitch fibres (Kaasik et al. 2003; Novotova et al. 2006). Furthermore, both MM-$CK^{-/-}$ and $CK^{-/-}$ mice showed worse voluntary exercise performance, relative to wild-type mice (Lygate et al. 2009; Momken et al. 2005). Muscles that can no longer function properly with regard to energy reserves and buffer systems adapt (at least partly) by increasing their oxidative and glycolytic potentials and by operating in a tense-flow mode (Veksler et al. 1995; Ventura-Clapier et al. 2004). For heart, it has been proposed that the increase in cardiac work become more “energetically costly” when the activity of the CK falls below a certain level (Saupe et al. 1998) and it seems that lack of Mt-CK induces lower MM-CK activity in heart (Boehm et al. 1998).

Mt-$CK^{-/-}$ mice have been less frequently studied than MM-$CK^{-/-}$ and $CK^{-/-}$ mice because their phenotype is less abnormal. At the age of 3 months, Mt-$CK^{-/-}$ mice and control mice shown similar levels of performance in a moderate- and high-intensity incremental exercise test (Miotto and Holloway 2016). However, Lygate and al. (2009) showed that older (7- to 8-months) Mt-$CK^{-/-}$ mice had a lower voluntary exercise capacity (Lygate et al. 2009); this could be related to the fact that at 7-8 months PCr and ATP levels were reduced while ADP level was increased in the left ventricle, despite normal cardiac phenotype and function parameters measured (Spindler et al. 2002), therefore that Mt-CK is necessary for normal metabolic homeostasis.

Hence, the objectives of the present work were to assess the performance of 6-, 9- and 18-months (mo) Mt-CK$^{-/-}$ male mice in an incremental exercise test and to characterize the associated age-related metabolic adaptations. Furthermore, we hypothesized that ageing contribute to impairments in mitochondrial biogenesis and mitochondria dynamics. It is well known that mitochondria are highly dynamic organelles and are constantly being remodelled by biogenesis, fusion, and fission. Alterations in mitochondria dynamics contribute to impairment energy generation and more recently, studies proposed that alteration of mitochondrial dynamic factors could affect muscle atrophy (Romanello et al. 2010; Tezze et al. 2017). It appears that mitochondrial dynamics change with age, even though causes, regulation mechanisms and consequences of these processes have not been elucidated (Liu et al. 2020). Indeed, the MM-CK$^{-/-}$ mouse displays high levels of citrate synthase (CS) activity in glycolytic skeletal muscle and higher mRNA expression levels of the mitochondrial fission factor dynamin-related protein 1 (Drp-1) (Vaarmann et al. 2008). We therefore investigated the mitochondrial factors involved in mitochondrial biogenesis and dynamics in the skeletal muscle (quadriceps) of Mt-CK$^{-/-}$ mice.

2. Material and method

2.1 Animals

The Mt-CK$^{-/-}$ mice had a mixed C57Bl/6–129/Sv background and were produced from heterozygous mice donated by Professor Stefan Neubauer laboratory's (Department of Cardiovascular Medicine, University of Oxford, Oxford, UK). These mice were originally created in Professor Bé Wieringa's laboratory (Nijmegen University, Nijmegen, The Netherlands) (Steeghs et al. 1998). Breeding was monitored in an animal facility. The mice were produced by heterozygous mating and the Mt-CK$^{-/-}$ and Mt-CK$^{+/+}$ offsprings were used for experimentation. The mice were genotyped to confirm sarcomeric ablation of the Mt-CK isoenzyme, using the protocol described by the originating laboratory (Nahrendorf et al. 2005). A total of 72 male mice

were obtained: 38 Mt-CK$^{-/-}$ mice and 34 control mice Mt-CK$^{+/+}$ The two types were divided into three age groups, referred to henceforth as 6-mo, 9-mo, and 18-mo. These mice were housed (in subgroups of three or four per cage) in a specific and opportunistic pathogen-free environment at a temperature of 22°C, with 12-hour light-dark cycles and a standard *ad libitum* diet.

All protocols were approved by our institution's Animal Care and Use Committee and complied with the Council of Europe's convention on the protection of vertebrate animals used for experimental and other scientific purposes.

2.2 The incremental exercise test

All groups underwent an incremental exercise test on a treadmill with a slope of 0° or 25°. Before testing, all mice were familiarized with the one-lane treadmill equipped for gas exchange measurements (Modular Enclosed Metabolic Treadmill for Mice, Columbus Instruments, Columbus, OH, USA) over a one-week period. The familiarization started on the first day at 0 m.min^{-1} for 10 minutes, and then with a 10-min run at 3 m.min^{-1}. On day 2, the mice ran at 3 m.min^{-1} for 5 min and then at 6 m.min^{-1} for 5 min. On day 3, they ran at 6 m.min^{-1} for 10 minutes. On day 4, they ran at 6 m.min^{-1} for 5 min and then at 10 m.min^{-1} for 5 min. Lastly, on day 5, the mice ran at 10 m.min^{-1} for 10 min. After 48h the mice underwent the test at 0° and then the same mice were tested after one week at 25°.

In the test, the mice were first recorded at rest for 8 min. The mice then started to run at 10 m.min^{-1}, and the treadmill velocity was then increased by 3 m.min^{-1} every 3 min until the mice were exhausted (defined as the moment when the mouse was in contact with the electric grid for 5 seconds). Gas samples were taken every 5 seconds and dried prior to measurement of the oxygen fraction with a gas analyser (Columbus Instruments). Oxygen uptake (VO_2) was calculated as described previously (Ayachi et al. 2016; Taylor et al. 1981). To enable a comparison with

human data, VO_2 was expressed relative to the BW raised to the power 0.75 (supplementary figure).

We presented the absolute highest oxygen consumption (VO_2peak) values and VO_2peak/HW ratio, since the oxygen consumption capacity and the cardiac output are directly related (according to the Fick equation: $Q = \dot{V}O_2$/a-vO2 difference).

Performance was evaluated as the maximum running speed (Vpeak). The blood lactate concentration was measured in a drop of blood from the tail vein 5 minutes after each incremental test, using the Lactate Pro LT-1710 meter (ARKRAY Europe, B.V., Amstelveen, the Netherlands). For exercise with a 25° slope, only those results that differed from the 0° slope setting are presented.

2.3 Mice sacrifice and sampling

Forty-eight hours after the last incremental exercise test, mice were sacrificed by intraperitoneal infusion of sodium pentobarbital (100 mg/kg; Sanofi Santé Animale, Paris, France). Samples of urine, heart muscle, skeletal muscles (the gastrocnemius, EDL, soleus, TA, and quadriceps) and liver were collected. The absolute weights of all skeletal muscles were normalized against the BW. We used the quadriceps of one leg for enzyme activity assays and the quadriceps of the other leg for Western blots. The urine samples were directly syringed from the bladder. All samples were stored at −80°C prior to analysis.

2.4 Enzyme assays

The quadriceps were weighed, homogenized (50 mg wet weight per 1 ml) in ice-cold buffer containing HEPES 5 mM (pH 8.7), EGTA 1 mM, dithiothreitol 1 mM and Triton X-100 (0.1%), and incubated for 60 min at 4 °C for complete enzyme extraction. The total activities of CK and CS were assayed (30 °C, pH 7.5) with coupled enzyme systems, as described previously (De Sousa et al. 2000). Citrate synthase activity was measured in terms of the production of 2-

nitro-5-thiobenzoate (measured spectrophotometrically at 412 nm) by the reaction between 5',5'-dithiobis-2- nitrobenzoic acid and CoA-SH. Total adenylate kinase and CK activities were determined using a coupled glucose-6-phosphate dehydrogenase/hexokinase enzyme assay, which produced NADPH (measured spectrophotometrically at 340 nm).

2.5 Western blots

The quadriceps muscles were homogenized in CelLytic™ MT Cell Lysis Reagent (Sigma-Aldrich, France) and then centrifuged at 11000 rpm (15000g) for 15 min at 4°C. The supernatant was removed and protease inhibitor cocktail was added. The protein concentration was quantified in a Bradford assay. Samples were denatured in SDS Laemmli 2× concentrate (Sigma-Aldrich) at 90°C for 5 min. Next, 10 µg aliquots of protein in 30 µl were loaded into each well of an SDS polyacrylamide gel (12%). The same protein standards were loaded on all gels to avoid variations from one membrane to another. The gels were run with running buffer at 140 V for 1 hour and then transferred onto a nitrocellulose membrane (pore size: 0.2 µm). After staining with Ponceau S reagent, the membranes were blocked with 5% bovine serum albumin (BSA) in Tris-buffered saline containing 0.1% Tween-20 (TBST) for 1 hour. The membranes were incubated with primary antibodies overnight at 4°C. The following primary antibodies were purchased from Cell Signaling (Netherlands) and Abcam (France) and were diluted in TBST-BSA: Mfn2 rabbit mAb (9482 Cell Signaling), 80 kDa dilution 1:1000; OPA-1 Rabbit mAb (80471 Cell Signaling), 80-100 kDa, 1:1000, Drp-1 rabbit mAb, 78-82 kDa (8570 Cell Signaling)dilution 1:1000; β-actin rabbit mAB (horse radish peroxidase (HRP) conjugate), 45 kDa, 1:1000 and PGC-1α-N-terminal rabbit polyclonal 91 kDa (ab54481 abcam), 1 µg/ml TBST-BSA. Anti-rabbit HRP-conjugated secondary antibody (Sigma Aldrich) diluted 1:10 000 in TBST-BSA was used to detect the primary antibodies. All protein expressions were normalized against β-actin (5125 Cell Signaling).

The membranes were then incubated with secondary antibodies (anti- rabbit Sigma) for 1 hour at room temperature and then washed in TBST four times prior to incubation with the secondary antibody for 1 hour at room temperature. The bands were detected using an enhanced chemiluminescence detection reagent kit (Bio-Rad France). Densitometry was performed using a Fusion imaging system (Viber Lourmat Deutschland GmbH, Eberhardzell, Germany).

2.6 NMR spectrometry

Urine samples were thawed at room temperature. A 100 µL aliquot of urine QS 600 µL PBS/D_2O was placed in a 5 mm NMR tube. An aliquot of D_2O (for field locking) was placed in the capillary tube holder. The proton spectra were acquired at 600 MHz on a Bruker Avance spectrometer (Bruker, France), with a reversed cryoprobe. The temperature was set to 294 K. The free induction decays (FIDs) were acquired using a NOESY1D sequence for water suppression, with a preacquisition delay of 2 seconds, a 100 ms mixing time, and a 90° pulse. The FIDs were collected to 64K complex points in a spectral window of 6600 Hz and 64 transients, after four silent scans. The FIDs were processed with NMRpipe software (Delaglio et al. 1995). The dataset was Fourier-transformed with an exponential function, producing 1 Hz line broadening. The spectra were phased, and the baseline was corrected using the segment method and three points at 0, 5, and 9 ppm. Each dataset was calibrated using the creatinine signal at 3.05 ppm. The spectrum between 0 ppm and 9.5 ppm was divided into 9500 spectral buckets of 0.001 ppm, using an in-house program written with R software. Each bucket was labelled with its median chemical shift value. The water region (between 4.6 and 5 ppm) was excluded from the data matrix. The bucket intensities were normalized using the probabilistic quotient technique (Meyer and Peters 2003) to obtain the X matrix for statistical analysis. Unit variance scaling was performed on all variables prior to a multivariate statistical analysis, and

spectra were aligned using the icoshift method (Savorani et al. 2010) to correct for the effect of pH on the metabolites' chemical shifts.

2.7 Statistical analyses

Statistical analyses were performed using SigmaStat software (version 3.5). Different age or genotype groups were compared in a two-way analysis of variance followed by a Student-Newman-Keuls post-hoc test. Whenever the normality test did not pass, for type effect we used Mann-Whitney analysis and for age a Kruskal-Wallis by ranks analysis was performed.

Multivariate statistical analysis

An unsupervised principal component analysis and a supervised orthogonal projection on latent structure (OPLS) analysis were performed using an in-house MATLAB routine (The MathWorks, Natick, MA, USA) based on the method described by Trygg and Wold (Trygg and Wold 2002). The principal component analysis was first applied to the X matrix data, in order to detect any separation between groups on the basis of the NMR signal variability. The O-PLS analysis was performed to identify differences between sample spectra as a function of the type of mice (control vs. Mt-CK$^{-/-}$). A model was computed for each age group (i.e. 6-, 9- and 18-mo). The quality of the O-PLS model was assessed by calculating the R2Y fit parameter (the variance explained) and the Q2Y cross-validated coefficient (the model's predictability). In our cases, only the model obtained with 6-mo mice urine samples gave satisfactory, valid R2Y and Q2Y parameters. A score plot and a loading plot were computed to illustrate the results of the O-PLS model. Each point in the score plot represented the projection of an NMR spectrum on the model's predictive component. The metabolites responsible for the classification obtained in the score plot were taken into account when their correlation coefficients between the NMR data and the model were higher than 0.5. In this case, these metabolites were considered as

discriminant metabolites. A heatmap summarizes these results, considering the discriminant metabolites only.

Results

3.1 Body weight and organ weights

The control and Mt-CK$^{-/-}$ groups did not differ with regard to body weight (BW) at 6 and 9 mo. However, at 18 months of age, the BW was 19% higher ($p<0.001$) in the control group than in the Mt-CK$^{-/-}$ group (Figure 1A). The BW was respectively 27% ($p<0.001$) and 21% higher in the 18-mo control group when compared with the 6-mo and 9-mo groups. When considering both types of mouse, a significant effect of age on BW ($p <0.001$) and a significant interaction between age and type ($p<0.001$) were seen (Figure 1A).

In both types of mouse, the absolute weight of the heart (Figure 1B) was significantly higher in the 18-mo group than in the 6-mo ($p<0.001$) and 9-mo ($p<0.001$) groups. However, once the heart weight (HW) was normalized to BW (Figure 1B), only the 18-mo Mt-CK$^{-/-}$ group had a significant higher value than the 6-mo Mt-CK$^{-/-}$ group ($p<0.001$) and the 9-mo Mt-CK$^{-/-}$ group ($p<0.001$). Furthermore, the ratio of HW/BW was significantly higher in the 18-mo Mt-CK$^{-/-}$ group than in the 18-mo control group ($p<0.01$). An overall effect of age was seen for both types at 6 months ($p=0.03$) and 9 months ($p=0.016$), relative to 18 months. Furthermore, the interaction between age and type was highly significant ($p=0.002$).

The absolute weight of EDL and TA did not differ by age or type, and only soleus weight was significantly lower in 18-mo Mt-CK$^{-/-}$ mice than in 18-mo control mice ($p<0.05$) (Table 1). Once the soleus weight was normalized against BW (Figure 1C), a significant effect of age ($p<0.001$) was detected. Moreover, the soleus/BW ratio was significantly lower ($p<0.001$) in 6-mo Mt-CK$^{-/-}$ mice than in 6-mo control mice. Age had no impact on the soleus weight in the Mt-CK$^{-/-}$ groups. In contrast, the soleus/BW ratio was significantly lower in the 9-mo ($p<0.05$) and

18-mo ($p<0.001$) control groups than in the 6-mo control group. A significant age-type interaction was detected for the soleus/BW ratio ($p=0.012$). This difference is mainly related to the absence of BW gain in the oldest group of Mt-CK$^{-/-}$ mouse.

Once the EDL weight was normalized against BW (Figure 1C), a significant age effect appeared ($p<0.001$). Furthermore, the EDL weight was lower in the 6-mo Mt-CK$^{-/-}$ group than in the 6-mo control group ($p<0.05$). The EDL/BW ratio was significantly lower in the 9-mo control ($p<0.05$) and 18-mo control ($p<0.001$) groups than in the 6-mo control. Age had no impact on the EDL/BW ratio in Mt-CK$^{-/-}$ mice.

The ratio of TA weight on BW (Figure 1C) was lower in 6-mo Mt-CK$^{-/-}$ mice than in 6-mo control mice ($p<0.05$). In control mice, the TA/BW ratio in 9-mo and 18-mo control mice were lower when compared to 6-mo control ($p<0.01$ at 9-mo; $p<0.001$ at 18-mo), while for Mt-CK$^{-/-}$, the TA/BW ratio remained unaffected by age. However, the interaction between age and type was significant ($p=0.032$).

In overall, for all skeletal muscles/BW ratio, the difference between control and Mt-CK$^{-/-}$, were only observed at 6-mo and not between 9 or 18-mo mice.

Finally, to make sure that ageing had no impact on the liver as an important organ for the regulation of glucose and lipid homeostasis, and in parallel to our metabolomics analysis, we measured the liver weight and controlled the general appearance. Comparison of absolute liver weight and liver weight/BW ratio showed no significant differences between mice types and between different ages in Mt-CK$^{-/-}$ mice. However, in control mice, the absolute liver weight was higher in 18-mo mice (1957.3 ± 122.5) than in 6-mo (1466.27 ± 116) and 9-mo (1349.7 ± 122.5) mice ($p<0.01$ for both). This difference disappeared once the liver weight was normalized on BW.

3.2 VO_2peak & performance

VO_2peak

We measured the maximal oxygen uptake (VO_2peak) with 0° and 25° slopes, as an index of the mice aerobic capacity. In the control mice, the absolute VO_2peak ($L.min^{-1}$) was higher in the 18-mo group than in the 6- and 9-mo groups (Figure 2A). When comparing the absolute VO_2peak (Figure 2 A) in the two types of mice of the same age, VO_2peak value was significant lower for 18-mo Mt-$CK^{-/-}$ mice ($p<0.001$) than for 18-mo controls. There was a significant effect of age in both control and Mt-$CK^{-/-}$ mice ($p=0.026$ at 0°).

At both slopes the VO_2peak/BW ratio (Figure 2B) was lower in the 18-mo Mt-$CK^{-/-}$ group than in the 6 and 9-mo Mt-$CK^{-/-}$ groups; however, no difference was detected between 18-mo control and Mt-$CK^{-/-}$ at the same age. This might also be related to the absence of BW gain in the oldest group of Mt-$CK^{-/-}$ mouse.

Furthermore, when VO_2peak was normalized to HW, the VO_2peak/HW ratio was 27% ($p<0.001$) lower in the 18-mo Mt-$CK^{-/-}$ group than in the 18-mo control group. Moreover, The VO_2peak /HW ratio was 29% ($p<0.001$) lower in 18-mo Mt-$CK^{-/-}$ mice than in 6-mo ($p<0.001$) and 32% ($p<0.001$) than 9-mo Mt-$CK^{-/-}$ mice (Figure 2C).

Maximal speed (Vpeak)

With a slope of 0° and 25° no differences were found between types of the same age. At 0° slope, there were no age differences in Vpeak among the control mice. However, Vpeak was 13% lower ($p<0.05$) in the 18-mo Mt-$CK^{-/-}$ group than in the 6-mo Mt-$CK^{-/-}$ group (Figure 3A). With a slope of 25°, the Vpeak was 22% lower ($p<0.05$) in the 18-mo group than in the 6-mo group for both control and Mt-$CK^{-/-}$ mice (Figure 3 B). Likewise, the Vpeak in the 18-mo groups was lower than in the 9-mo groups (Figure 3B). Hence, a significant effect of age was present at both slopes ($p=0.012$ at 0° and $p=0.001$ at 25°).

3.3 Blood lactate level 5 minutes after the incremental test

To evaluate the mice's recovery after the incremental test, we measured the clearance of accumulated blood lactate during 5 min of recovery after the end of the exercise bout. With a treadmill slope of 0°, the blood lactate concentration was significantly lower in the Mt-CK$^{-/-}$ group than in the control group at the age of 9 months ($p<0.05$) and 18 months ($p<0.01$). The blood lactate concentration was significantly higher in the 18-mo control group than in the 6-mo control group ($p=0.001$) and the 9-mo control group ($p<0.05$). In contrast, blood lactate did not appear to be related to age in the Mt-CK$^{-/-}$ mice (Figure 4). Hence, we observed an overall significant effect of age ($p=0.021$) and genotype ($p<0.001$), and an interaction between age and type ($p=0.03$) (Figure 4 A). The differences seen at a slope of 0° were not detected at a slope of 25° (Figure 4B).

3.4 Citrate synthase, creatine kinase and adenylate kinase activity in skeletal muscle

The enzyme activities in extracts from frozen quadriceps were determined spectrophotometrically. The assay results showed that neither age nor genotype influenced the activity values (Table 2). An analysis of the total CK activity in the quadriceps only revealed a significant interaction between age and genotype ($p= 0.048$).

3.5 Metabolomic

In an analysis of the urine metabolome, the OPLS-based comparison of the Mt-CK$^{-/-}$ group and the control group (Figure 5 A) showed that the R2Y and Q2Y values (0.980 and 0.771, respectively) were acceptable in 6-mo mice only. There was no control vs. Mt-CK$^{-/-}$ differences in mice at 9-mo or 18 mo. The discriminant metabolites responsible for this classification are represented as a heatmap (Figure 5B) showing that one of the most discriminant metabolites were branched-chain amino acids (BCAA) with other amino-acids such as glutamate and lysine. On the opposite, alanine was less eliminated in the urine of Mt-CK$^{-/-}$ when compared to control

mice. Besides, several other metabolites demonstrate that these two genotypes differ also from a metabolic thus phenotypic point of view.

3.6 Mitochondrial dynamics

The Western blot analysis showed that PGC-1α expression in the quadriceps muscle was lower in 18-mo control and Mt-CK$^{-/-}$ mice than in the corresponding 6-mo groups. An effect of age was detected (p= 0.021) (Figure 6A). There was also an overall effect of age on Mfn-2 expression in the quadriceps (p=0.017); expression of Mfn-2 in the quadriceps was significantly higher in the 18-mo groups than in the 6-mo groups (p=0.013) and the 9-mo groups (p=0.034) (Figure 6 B). A *post hoc* test revealed that the expression of Mfn-2 in the skeletal muscle of 18-mo Mt-CK$^{-/-}$ was significantly higher than in both the 6-mo Mt-CK$^{-/-}$ mice ($p<0.01$) and the 9-mo Mt-CK$^{-/-}$ mice ($p<0.05$). The expression of OPA-1 and Drp-1 in the quadriceps remained the same in both types of mouse and for all ages (6 C, D).

3. Discussion

Taken as a whole, the present study showed ageing is potentialized by Mt-CK deficiency with regard to VO2peak, Vpeak and mitochondrial protein expression. The Vpeak for18-mo Mt-CK$^{-/-}$ mice decreased at 0° and 25° while for control group of the same age the Vpeak decreased only at 25°. The main effects of genotype included a smaller BW gain with age and a greater HW/BW in Mt-CK$^{-/-}$ mice than in control mice. The skeletal muscle weights/BWs were lower in 6-mo Mt-CK$^{-/-}$ mice than in 6-mo control. In the same line, the metabolites eliminated in urine (notably higher levels of BCAAs) discriminated between Mt-CK$^{-/-}$ mice from control mice at the age of 6 months only. It is noteworthy that the Mt-CK$^{-/-}$ and control groups did not differ with regard to levels of lipid metabolites.

Although we did not measure energy expenditure or body temperature in the present study, research on other models related to creatine metabolism such as mice lacking creatine

394 transporters (SLC6A8), guanidinoacetate methyltransferase (GAMT) or CK KO mice (lacking brain-
395 type CK and mitochondrial ubiquitous CK) displayed a low BW, muscle weakness, muscle
396 atrophy, low amounts of white adipose tissue or impaired body temperature maintenance (Kan
397 et al. 2005; Russell et al. 2014; Stockebrand et al. 2018; Streijger et al. 2009). In addition, as it
398 was aforementioned, the increase in cardiac work become more “energetically costly” when the
399 activity of the CK fall below a certain level (Saupe et al. 1998) and it seems that lack of Mt-CK
400 induces lower MM-CK activity in heart (Boehm et al. 1998), that might explain a higher substrate
401 utilisation by heart in Mt-CK$^{-/-}$ mice.

402 The absolute HWs were significantly greater in both control and Mt-CK$^{-/-}$ mice at 18
403 months of age than at 6 and 9 months of age. After normalization against the BW, this difference
404 disappeared for control mice but remained for Mt-CK$^{-/-}$ because of the absence of BW gain.
405 Lygate et al. (2009) showed that Mt-CK$^{-/-}$ mice had normal cardiac function; hypertrophy was
406 not detected at the age of 20 to 40 weeks (Lygate et al. 2009). However, the Mt-CK$^{-/-}$ mice had a
407 higher heart rate (Lygate et al. 2009), and it has been reported that Mt-CK is required to maintain
408 normal high energy phosphate metabolite levels in heart (Spindler et al 2002).

409 With a treadmill slope of 0°, the absolute values of VO_2peak were the same in all Mt-CK$^{-/-}$
410 age groups. However, this was not the case for control mice, where the absolute VO_2peak was
411 higher at the age of 18 months than at 6 and 9 months. This might correspond to a response or
412 adaptation to a higher BW. We decided to normalize the VO_2peak against HW because the BW
413 curves differed for controls vs. Mt-CK$^{-/-}$ mice while the absolute HWs followed the same pattern
414 in both types of mouse. Once VO_2peak was normalized against HW, the VO_2peak/HW ratio with
415 treadmill slopes of 0° and 25° were significantly lower for 18-mo Mt-CK$^{-/-}$ mice than in 18-mo
416 control mice and in 6-mo and 9-mo Mt-CK$^{-/-}$ mice. We hypothesize that even after cardiac

adaptation at 18 months of age, the oldest Mt-CK$^{-/-}$ mice presented a lower aerobic capacity (as indicated by the VO_2peak value).

We observed a significant effect of age on Vpeak at slopes of 0° and 25°. However, the difference at 0° was mainly related to a lower Vpeak in 18-mo Mt-CK$^{-/-}$ than in 6-mo mice, which might be related to a greater age-related decline in performance in the Mt-CK$^{-/-}$ mice. With a 25° slope, the two genotypes showed the same decline in Vpeak with ageing. Our results are in line with Miotto and Holloway's (2016) report on run times to exhaustion in younger (4-month-old) control and Mt-CK$^{-/-}$mice with treadmill slopes of 5° and 20° (Miotto and Holloway 2016). However, in a study of voluntary wheel running over 3 weeks, Lygate et al. (2009) found that Mt-CK$^{-/-}$ mice aged 30 weeks performed less well than control mice (Lygate et al. 2009). This might have been related to the level of motivation of Mt-CK$^{-/-}$ mice, which opens up perspectives for the behavioural evaluation of this strain.

The two types of mouse differed with regard to the age-related change in blood lactate during the incremental test with a 0° slope (i.e. an age-type interaction). The blood lactate concentration was significant lower in the 9-mo and 18-mo Mt-CK$^{-/-}$ mice than in the corresponding control groups. This difference disappeared when the slope was 25°, that is more comparable to the results found by Miotto et al (2016), comparing 12 weeks Mt-CK$^{-/-}$ mice blood lactate with wild type mice after exhaustive exercise (Miotto and Holloway 2016) . For the 18-mo Mt-CK$^{-/-}$ mice, the lower blood lactate might be related to lower performance or less work load because of lower body weight. However, the two types of mouse achieved the same maximal speed at 9 months of age but the blood lactate level was lower in the 9-mo Mt-CK$^{-/-}$ group. The lower blood lactate level in Mt-CK$^{-/-}$ mice might be also related to adaptation of the heart in order to compensate for the energy deficit; the Mt-CK$^{-/-}$ heart tissue might use a higher concentration of lactic acid than the heart tissue of control mice at the same age. Consequently,

441 the Mt-CK$^{-/-}$ mice might have a more efficient lactate uptake system, as has been shown in some
442 tissues (such as the liver) in starved mice (Schutkowski et al. 2014). In addition, probably these
443 mice had other compensatory adaptations, such as increasing the production of ATP through the
444 cofactor nicotinamide adenine dinucleotide (NAD^+) production to boost oxidative
445 phosphorylation, that needs further studies in Mt-CK$^{-/-}$ mice. Further, as metabolomic results
446 (discussed below) showed the Mt-CK$^{-/-}$ at 6mo, had increased BCAAs, glutamate and lysine in
447 urine while alanine was less present in the urine of the 6-mo Mt-CK$^{-/-}$ mice, probably suggesting
448 that alanine was mainly converted to pyruvate through gluconeogenesis.

449 The presence of methionine (an anabolic stimulant) and BCAAs and other amino acids in
450 the urine of 6-mo Mt-CK$^{-/-}$ mice (compared with 6-mo control mice) might suggest an imbalance
451 in protein turnover, i.e. more protein catabolism rather than protein anabolism in these animals.
452 These Mt-CK$^{-/-}$ vs. control differences were not detected at the ages of 9 and 18 months, and the
453 difference appeared to have been lost with age. Protein turnover may lead to protein catabolism
454 to a similar extent in both the Mt-CK$^{-/-}$ and control mice at 9 and 18 months of age. Other
455 studies have suggested that muscle mass loss during ageing is due to impairment of the cell's
456 energy status (Hiona et al. 2010; Neelakantan et al. 2019; Nuss et al. 2009; Tepp et al. 2016). At
457 11 months of age, a mouse model of premature ageing (the mitochondrial DNA polymerase γ
458 knock-out mouse) displays the degree of skeletal muscle sarcopenia usually observed at the age
459 of 30 months in control mice. This sarcopenia was associated with low levels of electron
460 transport chain complex components and impaired mitochondrial bioenergetics (Hiona et al.
461 2010).

462 The protein expression of factors involved in mitochondrial biogenesis and dynamics in
463 the quadriceps revealed an effect of age. We found that in both types of mouse, protein
464 expression of PGC-1 was lower at 18 months of age and protein expression of Mfn-2 was higher

465 at 18 months of age than in younger counterparts. The expression of Opa1 did not differ with
466 age, and we did not observe any differences of Drp-1 expression as a function of genotype or
467 age. The impact of ageing on muscle mitochondrial content is subject to debate (Chabi et al.
468 2008; Lanza and Nair 2009; Leduc-Gaudet et al. 2015). Indeed, protein synthesis is an
469 energetically demanding process. A number of studies suggest that alterations in mitochondrial
470 function and structure (i) are involved in sarcopenia and the loss of muscle function during
471 ageing, and (ii) start before muscle sarcopenia becomes apparent (Del Campo et al. 2018;
472 Figueiredo et al. 2009; Joseph et al. 2013). Our results showed that ageing impacts the protein
473 expression of PGC-1α , as has been observed in skeletal muscle from older adults (Joseph et al.
474 2012). This probably suggests that mitochondrial biogenesis in the quadriceps was lower in the
475 18-mo group than in the younger mice. Furthermore, greater skeletal muscle levels of both Mfn1
476 and Mfn2 were reported in elderly mice and monkeys (Mercken et al. 2017). However, Leduc-
477 Gaudet et al. (2015) reported that ageing does not alter the expression levels of proteins related
478 to mitochondrial fission or fusion (Leduc-Gaudet et al. 2015). Nevertheless, they observed a
479 higher Mfn2/Drp-1 ratio in the skeletal muscle of older mice (Leduc-Gaudet et al. 2015). It is
480 possible that with age, adaptation of mitochondria in the skeletal muscles (through fusion and
481 fission) is more prominent than mitochondrial biogenesis.

482 It has been reported that muscle disuse is associated with lower levels of the inner and
483 outer mitochondrial membrane fusion factors Mfn2 and Opa1 (Tezze et al. 2017). Furthermore,
484 the overexpression of Drp-1 is reportedly involved in skeletal muscle atrophy and muscle disuse
485 in mice (Romanello et al. 2010). However, we did not find intergroup differences in Drp-1
486 expression in the quadriceps. In contrast, other studies reported the overexpression of Drp-1 in
487 the gastrocnemius muscle of 9-mo rats (Faitg et al. 2019) . It is probable that not all muscle types
488 age at the same speed (Crupi et al. 2018).

The skeletal muscle enzyme activity assay did not reveal any significant differences in total CK and citrate synthase activities. However, a significant interaction between age and type was observed. This might be related to compensation by MM-CK in Mt-CK$^{-/-}$ mice. However, we did not measure the enzyme activity in skeletal muscles other than the quadriceps that is a mixed muscle. Lygate and al. showed that Mt-CK$^{-/-}$ mice at 30 weeks, had higher MM-CK activity in the soleus muscle but not in glycolytic (gastrocnemius) muscle (Lygate et al. 2009). The higher expression of MM-CK might be in favour of maintaining muscle power, and probably the reason that at 6 mo and 9 mo the Mt-CK$^{-/-}$ mice present the same performance as control mice; however, this compensation might not be enough at older age.

A large body of evidence shows that the CK phosphotransfer pathway in rodent heart and skeletal muscle becomes significantly less efficient with age (Kanski et al. 2005; Nuss et al. 2009; Tepp et al. 2017; Tepp et al. 2016). On the same lines, most of our results suggest that the effect of age was greater than the effect of genotype. The observed effect of genotype and the presence of a lower BW and higher HW in Mt-CK$^{-/-}$mice suggest that physiological adaptations enable the KO mice to maintain the same level of performance as control mice. However, the fact that VO_2peak and Vpeak are lower in older Mt-CK$^{-/-}$ mice than in younger Mt-CK$^{-/-}$ mice suggests that this strain ages more quickly than control mice. In future research, it would be interesting to use the cre-lox system to create targeted Mt-CK$^{-/-}$ mice and this to avoid the physiological adaptations that are present in most transgenic mice. It would also be interesting to perform the same study in Mt-CK$^{-/-}$ at older age such as 24 months.

The present study had several strengths, this was the first time that the performance of Mt-CK$^{-/-}$ mice had been evaluated at such an advance age (18 months). A relatively large number of mice were used. The study also had several limitations. Firstly, we did not normalize the organ weight against the length of the tibia bone. Secondly, we did not measure energy expenditure

and cardiac function. Finally, the protein assays and enzyme activity assay were performed on the quadriceps only. In future research, it would be better to study these parameters in the heart and in a broader range of skeletal muscles. These observations might provide more information on putative adaptation mechanisms during ageing in Mt-CK$^{-/-}$ mice.

4. Conclusion

In conclusion, the present study showed ageing is potentialized by Mt-CK deficiency with regard to VO2peak, Vpeak and mitochondrial protein expression. The genotype effect in our study were mainly reflected in smaller BW gain, a greater HW/BW in Mt-CK$^{-/-}$ mice through ageing. The skeletal muscle weights/BW and urine metabolomics analysis could explain protein wasting in these mice at younger age when compared to their counterparts in control but this difference disappeared at older age probably due to the loss of muscle mass in control mice. There is no doubt that Mt-CK$^{-/-}$ mice undergo physiological adaptations, enabling them to survive and to performance as well as wild-type mice. However, it is possible that these adaptations in Mt-CK$^{-/-}$ mice have a high energy cost and might trigger premature ageing. Studies of energy metabolism pathways would be required to confirm this.

Acknowledgment

We are sincerely acknowledging to Dr. Stefan Neubauer, Dr. Craig A. Lygate for donation of heterozygous Creatine kinase deficient mice, thank to Dr. Ventura-Clapier R, Pr. Veksler V for their remark and helpful discussion. We thank the master students: Abla MOUSSA, Yassemine Elberd, and Kopoin Deborah for their experimental contribution. We thank INRA for animal housing (IERP, INRA, 2018. Infectiology of fishes and rodent facility, doi:10.15454/1.5572427140471238E12).

Authors contribution statements

In the present study: Niel R: performed all the incremental exercise test and analyzed the data and participated in writing the manuscript. Le Moyec L: supervised all mice urine sample analysis by NMR and worked on the manuscript. Launay T: participated in experimentation and analysis of the western blots and worked on the manuscript. Hamard Mille L: supervised the incremental tests and worked on the manuscript. Triba MN: contributed to the statistical analysis of NMR data. Maciejak O: carried out the NMR experimentation. Billat V: developed the idea and worked on the manuscript. Momken I: conducted and directed the project, performed genotyping of mice and the enzyme activity assay and wrote the manuscript. All authors, discussed the results and the manuscript.

References

Ayachi, M., R. Niel, I. Momken, V.L. Billat and L. Mille-Hamard. 2016. Validation of a Ramp Running Protocol for Determination of the True VO2max in Mice. Front Physiol 7.

Bodyak, N., P.M. Kang, M. Hiromura, I. Sulijoadikusumo, N. Horikoshi, K. Khrapko and A. Usheva. 2002. Gene expression profiling of the aging mouse cardiac myocytes. Nucleic Acids Res 30: 3788-3794.

Boehm, E., V. Veksler, P. Mateo, C. Lenoble, B. Wieringa and R. Ventura-Clapier. 1998. Maintained coupling of oxidative phosphorylation to creatine kinase activity in sarcomeric mitochondrial creatine kinase-deficient mice. J Mol Cell Cardiol 30: 901-912.

Chabi, B., V. Ljubicic, K.J. Menzies, J.H. Huang, A. Saleem and D.A. Hood. 2008. Mitochondrial function and apoptotic susceptibility in aging skeletal muscle. Aging Cell 7: 2-12.

Crupi, A.N., J.S. Nunnelee, D.J. Taylor, A. Thomas, J.P. Vit, C.E. Riera, R.A. Gottlieb and H.S. Goodridge. 2018. Oxidative muscles have better mitochondrial homeostasis than glycolytic muscles throughout life and maintain mitochondrial function during aging. Aging (Albany NY) 10: 3327-3352.

De Sousa, E., V. Veksler, X. Bigard, P. Mateo and R. Ventura-Clapier. 2000. Heart failure affects mitochondrial but not myofibrillar intrinsic properties of skeletal muscle. Circulation 102: 1847-1853.

Del Campo, A., I. Contreras-Hernandez, M. Castro-Sepulveda, C.A. Campos, R. Figueroa, M.F. Tevy, V. Eisner, M. Casas and E. Jaimovich. 2018. Muscle function decline and mitochondria changes in middle age precede sarcopenia in mice. Aging (Albany NY) 10: 34-55.

Delaglio, F., S. Grzesiek, G.W. Vuister, G. Zhu, J. Pfeifer and A. Bax. 1995. NMRPipe: a multidimensional spectral processing system based on UNIX pipes. J Biomol NMR 6: 277-293.

Faitg, J., J.P. Leduc-Gaudet, O. Reynaud, G. Ferland, P. Gaudreau and G. Gouspillou. 2019. Effects of Aging and Caloric Restriction on Fiber Type Composition, Mitochondrial Morphology and Dynamics in Rat Oxidative and Glycolytic Muscles. Front Physiol 10: 420.

Figueiredo, P.A., S.K. Powers, R.M. Ferreira, H.J. Appell and J.A. Duarte. 2009. Aging impairs skeletal muscle mitochondrial bioenergetic function. J Gerontol A Biol Sci Med Sci 64: 21-33.

Hiona, A., A. Sanz, G.C. Kujoth, R. Pamplona, A.Y. Seo, T. Hofer, S. Someya, T. Miyakawa, C. Nakayama, A.K. Samhan-Arias, S. Servais, J.L. Barger, M. Portero-Otin, M. Tanokura, T.A. Prolla and C. Leeuwenburgh. 2010. Mitochondrial DNA mutations induce mitochondrial dysfunction, apoptosis and sarcopenia in skeletal muscle of mitochondrial DNA mutator mice. PLoS One 5: e11468.

Joseph, A.M., P.J. Adhihetty, T.W. Buford, S.E. Wohlgemuth, H.A. Lees, L.M. Nguyen, J.M. Aranda, B.D. Sandesara, M. Pahor, T.M. Manini, E. Marzetti and C. Leeuwenburgh. 2012. The impact of aging on mitochondrial function and biogenesis pathways in skeletal muscle of sedentary high- and low-functioning elderly individuals. Aging Cell 11: 801-809.

Joseph, A.M., P.J. Adhihetty, N.R. Wawrzyniak, S.E. Wohlgemuth, A. Picca, G.C. Kujoth, T.A. Prolla and C. Leeuwenburgh. 2013. Dysregulation of mitochondrial quality control processes contribute to sarcopenia in a mouse model of premature aging. PLoS One 8: e69327.
Kaasik, A., V. Veksler, E. Boehm, M. Novotova and R. Ventura-Clapier. 2003. From energy store to energy flux: a study in creatine kinase-deficient fast skeletal muscle. FASEB J 17: 708-710.
Kaczor, J.J., W. Ziolkowski, J. Antosiewicz, S. Hac, M.A. Tarnopolsky and J. Popinigis. 2006. The effect of aging on anaerobic and aerobic enzyme activities in human skeletal muscle. J Gerontol A Biol Sci Med Sci 61: 339-344.
Kaldis, P., G. Kamp, T. Piendl and T. Wallimann. 1997. Functions of Creatine Kinase Isoenzymes in Spermatozoa. pp. 275-312 in P.M. Wassarman, ed. Advances in Developmental Biology (1992). Academic Press.
Kan, H.E., T.E. Buse-Pot, R. Peco, D. Isbrandt, A. Heerschap and A. de Haan. 2005. Lower force and impaired performance during high-intensity electrical stimulation in skeletal muscle of GAMT-deficient knockout mice. Am J Physiol Cell Physiol 289: C113-119.
Kanski, J., S.J. Hong and C. Schoneich. 2005. Proteomic analysis of protein nitration in aging skeletal muscle and identification of nitrotyrosine-containing sequences in vivo by nanoelectrospray ionization tandem mass spectrometry. J Biol Chem 280: 24261-24266.
Lanza, I.R., and K.S. Nair. 2009. Muscle mitochondrial changes with aging and exercise. Am J Clin Nutr 89: 467s-471s.
Leduc-Gaudet, J.P., M. Picard, F. St-Jean Pelletier, N. Sgarioto, M.J. Auger, J. Vallee, R. Robitaille, D.H. St-Pierre and G. Gouspillou. 2015. Mitochondrial morphology is altered in atrophied skeletal muscle of aged mice. Oncotarget 6: 17923-17937.
Liu, Y.J., R.L. McIntyre, G.E. Janssens and R.H. Houtkooper. 2020. Mitochondrial fission and fusion: A dynamic role in aging and potential target for age-related disease. Mech Ageing Dev 186: 111212.
Lygate, C.A., I. Hunyor, D. Medway, J.P. de Bono, D. Dawson, J. Wallis, L. Sebag-Montefiore and S. Neubauer. 2009. Cardiac phenotype of mitochondrial creatine kinase knockout mice is modified on a pure C57BL/6 genetic background. J Mol Cell Cardiol 46: 93-99.
Mercken, E.M., M. Capri, B.A. Carboneau, M. Conte, J. Heidler, A. Santoro, A. Martin-Montalvo, M. Gonzalez-Freire, H. Khraiwesh, J.A. Gonzalez-Reyes, R. Moaddel, Y. Zhang, K.G. Becker, J.M. Villalba, J.A. Mattison, I. Wittig, C. Franceschi and R. de Cabo. 2017. Conserved and species-specific molecular denominators in mammalian skeletal muscle aging. NPJ Aging Mech Dis 3: 8.
Meyer, B., and T. Peters. 2003. NMR spectroscopy techniques for screening and identifying ligand binding to protein receptors. Angew Chem Int Ed Engl 42: 864-890.
Miotto, P.M., and G.P. Holloway. 2016. In the absence of phosphate shuttling, exercise reveals the in vivo importance of creatine-independent mitochondrial ADP transport. Biochem J 473: 2831-2843.
Momken, I., P. Lechene, N. Koulmann, D. Fortin, P. Mateo, B.T. Doan, J. Hoerter, X. Bigard, V. Veksler and R. Ventura-Clapier. 2005. Impaired voluntary running capacity of creatine kinase-deficient mice. J Physiol 565: 951-964.
Nahrendorf, M., M. Spindler, K. Hu, L. Bauer, O. Ritter, P. Nordbeck, T. Quaschning, K.H. Hiller, J. Wallis, G. Ertl, W.R. Bauer and S. Neubauer. 2005. Creatine kinase knockout mice show left ventricular hypertrophy and dilatation, but unaltered remodeling post-myocardial infarction. Cardiovascular research 65: 419-427.
Neelakantan, H., C.R. Brightwell, T.G. Graber, R. Maroto, H.L. Wang, S.F. McHardy, J. Papaconstantinou, C.S. Fry and S.J. Watowich. 2019. Small molecule nicotinamide N-methyltransferase inhibitor activates senescent muscle stem cells and improves regenerative capacity of aged skeletal muscle. Biochem Pharmacol 163: 481-492.
Nemutlu, E., A. Gupta, S. Zhang, M. Viqar, E. Holmuhamedov, A. Terzic, A. Jahangir and P. Dzeja. 2015. Decline of Phosphotransfer and Substrate Supply Metabolic Circuits Hinders ATP Cycling in Aging Myocardium. PLoS One 10: e0136556.
Novotova, M., M. Pavlovicova, V.I. Veksler, R. Ventura-Clapier and I. Zahradnik. 2006. Ultrastructural remodeling of fast skeletal muscle fibers induced by invalidation of creatine kinase. Am J Physiol Cell Physiol 291: C1279-1285.

Nuss, J.E., J.K. Amaning, C.E. Bailey, J.H. DeFord, V.L. Dimayuga, J.P. Rabek and J. Papaconstantinou. 2009. Oxidative modification and aggregation of creatine kinase from aged mouse skeletal muscle. Aging (Albany NY) 1: 557-572.
Pastoris, O., F. Boschi, M. Verri, P. Baiardi, G. Felzani, J. Vecchiet, M. Dossena and M. Catapano. 2000. The effects of aging on enzyme activities and metabolite concentrations in skeletal muscle from sedentary male and female subjects. Exp Gerontol 35: 95-104.
Romanello, V., E. Guadagnin, L. Gomes, I. Roder, C. Sandri, Y. Petersen, G. Milan, E. Masiero, P. Del Piccolo, M. Foretz, L. Scorrano, R. Rudolf and M. Sandri. 2010. Mitochondrial fission and remodelling contributes to muscle atrophy. Embo j 29: 1774-1785.
Russell, A.P., L. Ghobrial, C.R. Wright, S. Lamon, E.L. Brown, M. Kon, M.R. Skelton and R.J. Snow. 2014. Creatine transporter (SLC6A8) knockout mice display an increased capacity for in vitro creatine biosynthesis in skeletal muscle. Front Physiol 5: 314.
Saupe, K.W., M. Spindler, R. Tian and J.S. Ingwall. 1998. Impaired cardiac energetics in mice lacking muscle-specific isoenzymes of creatine kinase. Circ Res 82: 898-907.
Savorani, F., G. Tomasi and S.B. Engelsen. 2010. icoshift: A versatile tool for the rapid alignment of 1D NMR spectra. J Magn Reson 202: 190-202.
Schlattner, U., M. Dolder, T. Wallimann and M. Tokarska-Schlattner. 2001. Mitochondrial creatine kinase and mitochondrial outer membrane porin show a direct interaction that is modulated by calcium. J Biol Chem 276: 48027-48030.
Schlattner, U., M. Forstner, M. Eder, O. Stachowiak, K. Fritz-Wolf and T. Wallimann. 1998. Functional aspects of the X-ray structure of mitochondrial creatine kinase: a molecular physiology approach. Mol Cell Biochem 184: 125-140.
Schutkowski, A., N. Wege, G.I. Stangl and B. Konig. 2014. Tissue-specific expression of monocarboxylate transporters during fasting in mice. PLoS One 9: e112118.
Spindler, M., R. Niebler, H. Remkes, M. Horn, T. Lanz and S. Neubauer. 2002. Mitochondrial creatine kinase is critically necessary for normal myocardial high-energy phosphate metabolism. Am J Physiol Heart Circ Physiol 283: H680-687.
Steeghs, K., F. Oerlemans, A. de Haan, A. Heerschap, L. Verdoodt, M. de Bie, W. Ruitenbeek, A. Benders, C. Jost, J. van Deursen, P. Tullson, R. Terjung, P. Jap, W. Jacob, D. Pette and B. Wieringa. 1998. Cytoarchitectural and metabolic adaptations in muscles with mitochondrial and cytosolic creatine kinase deficiencies. Mol Cell Biochem 184: 183-194.
Stockebrand, M., A. Sasani, D. Das, S. Hornig, I. Hermans-Borgmeyer, H.A. Lake, D. Isbrandt, C.A. Lygate, A. Heerschap, A. Neu and C.U. Choe. 2018. A Mouse Model of Creatine Transporter Deficiency Reveals Impaired Motor Function and Muscle Energy Metabolism. Front Physiol 9: 773.
Streijger, F., H. Pluk, F. Oerlemans, G. Beckers, A.C. Bianco, M.O. Ribeiro, B. Wieringa and C.E. Van der Zee. 2009. Mice lacking brain-type creatine kinase activity show defective thermoregulation. Physiol Behav 97: 76-86.
Taylor, C.R., G.M. Maloiy, E.R. Weibel, V.A. Langman, J.M. Kamau, H.J. Seeherman and N.C. Heglund. 1981. Design of the mammalian respiratory system. III Scaling maximum aerobic capacity to body mass: wild and domestic mammals. Respir Physiol 44: 25-37.
Tepp, K., M. Puurand, N. Timohhina, J. Adamson, A. Klepinin, L. Truu, I. Shevchuk, V. Chekulayev and T. Kaambre. 2017. Changes in the mitochondrial function and in the efficiency of energy transfer pathways during cardiomyocyte aging. Mol Cell Biochem 432: 141-158.
Tepp, K., N. Timohhina, M. Puurand, A. Klepinin, V. Chekulayev, I. Shevchuk and T. Kaambre. 2016. Bioenergetics of the aging heart and skeletal muscles: Modern concepts and controversies. Ageing Res Rev 28: 1-14.
Tezze, C., V. Romanello, M.A. Desbats, G.P. Fadini, M. Albiero, G. Favaro, S. Ciciliot, M.E. Soriano, V. Morbidoni, C. Cerqua, S. Loefler, H. Kern, C. Franceschi, S. Salvioli, M. Conte, B. Blaauw, S. Zampieri, L. Salviati, L. Scorrano and M. Sandri. 2017. Age-Associated Loss of OPA1 in Muscle Impacts Muscle Mass, Metabolic Homeostasis, Systemic Inflammation, and Epithelial Senescence. Cell Metab 25: 1374-1389.e1376.

Trygg, J., and S. Wold. 2002. Orthogonal projections to latent structures (O-PLS). Journal of Chemometrics 16: 119-128.
Vaarmann, A., D. Fortin, V. Veksler, I. Momken, R. Ventura-Clapier and A. Garnier. 2008. Mitochondrial biogenesis in fast skeletal muscle of CK deficient mice. Biochim Biophys Acta 1777: 39-47.
van Deursen, J., A. Heerschap, F. Oerlemans, W. Ruitenbeek, P. Jap, H. ter Laak and B. Wieringa. 1993. Skeletal muscles of mice deficient in muscle creatine kinase lack burst activity. Cell 74: 621-631.
Veksler, V.I., A.V. Kuznetsov, K. Anflous, P. Mateo, J. van Deursen, B. Wieringa and R. Ventura-Clapier. 1995. Muscle creatine kinase-deficient mice. II. Cardiac and skeletal muscles exhibit tissue-specific adaptation of the mitochondrial function. J Biol Chem 270: 19921-19929.
Ventura-Clapier, R., A. Kaasik and V. Veksler. 2004. Structural and functional adaptations of striated muscles to CK deficiency. Mol Cell Biochem 256-257: 29-41.
Wallimann, T. 2015. The extended, dynamic mitochondrial reticulum in skeletal muscle and the creatine kinase (CK)/phosphocreatine (PCr) shuttle are working hand in hand for optimal energy provision. J Muscle Res Cell Motil 36: 297-300.
Ydfors, M., M.C. Hughes, R. Laham, U. Schlattner, J. Norrbom and C.G. Perry. 2016. Modelling in vivo creatine/phosphocreatine in vitro reveals divergent adaptations in human muscle mitochondrial respiratory control by ADP after acute and chronic exercise. J Physiol 594: 3127-3140.

Table Legend

Table 1: Anatomic data. For the two-way ANOVA and post hoc test: *p<0.05, **p<0.01, indicate a significant difference vs. controls of the same age; †p<0.05 and ††p<0.01 indicate a significant difference vs. the 6-mo group of the same genotype, and $$p<0.01, indicate a significant difference vs. the 9-mo group of the same genotype; Extensor digitorum longus (EDL), Anterior tibialis (TA).

Table 2. The quadriceps citrate synthase, creatine kinase and adenylate kinase activity, the enzymes activities are expressed in international unit per gram wet weight (IU/g WW).

Table 1.

	6 mo Cont n=12	6 mo Mt-CK$^{-/-}$ n=13	9 mo Cont n=11	9 mo Mt-CK$^{-/-}$ n=13	18 mo Cont n=10	18 mo Mt-CK$^{-/-}$ n=9	Interaction Age x type
Soleus (mg)	9.91±0.4	9.11±0.35	9.3±0.34	9.45±0.15	9.85±0.25	8.61±0.57*	------
EDL (mg)	10±0.38	9.09±0.37	9.13±0.42	9.45±0.42	9.56±0.47	8.43±0.66	------
TA (mg)	46.1±1.33	42.5±1.96	41.7±2.46	40.6±1.58	43.9±1.87	42.4±1.75	------

Table 2.

IU/g WW	**6 mo Cont n=7**	**6 mo Mt-CK$^{-/-}$ n=8**	**9 mo Cont n=8**	**9 mo Mt-CK$^{-/-}$ n=8**	**18 mo Cont n=7**	**18 mo Mt-CK$^{-/-}$ n=7**	**Interaction Age x type**
CS	681.9±28	757.3±15	678.5±18	737.2±20.5	697.9±23	656.7±17	0.059
Total CK	1118.6±53	1192.7±49.6	1064.15±49.6	1185±49.6	1190.9±53	1061.3±53	0.048

AK	838±31.5	852.5±29.4	827.85±29.4	835.35±29.4	870.3±31.5	830.65±31.5	0.641

Figure Legend

Figure 1. (A) Body weight at 6, 9 and 18 months of age; (B) Absolute heart weight (HW) and HW normalized to BW; (C) Skeletal muscles: Soleus, Extensor digitorum longus (EDL), Anterior tibialis (TA) normalised to body weight (BW). In the *post hoc* test, *p<0.05, **p<0.01 and ***p<0.001 indicate a significant difference vs. controls of the same age, †p<0.05, ††p<0.01, †††p<0.001 indicate a significant difference vs. the 6-mo group of the same genotype. The age-type interactions were apparent. 6-mo control n=12, 9-mo control n=10, 18-mo control n=10; 6-mo Mt-CK$^{-/-}$ n=13, 9-mo Mt-CK$^{-/-}$ n=13, 18-mo Mt-CK$^{-/-}$ n=9.

Figure 2. (A) Net VO_2peak at a slope of 0°. (B) VO_2peak/BW (C) VO_2peak/Heart weight (HW) at a slope of 0°. In a *post hoc* test; **p<0.01 ***p<0.001 indicates a significant difference vs. controls of the same age, †p<0.05, †††p≤0.001 indicates a significant difference vs. the 6-mo group of the same genotype and $p<0.05, $$p<0.01 and indicate a significant difference vs. the 9-mo group of the same genotype. 6-mo control n=12, 9-mo control n=10, 18-mo control n=10; 6-mo Mt-CK$^{-/-}$ n=13, 9-mo Mt-CK$^{-/-}$ n=13, 18-mo Mt-CK$^{-/-}$ n=8

Figure 3. Maximum running speed (Vpeak) (A) at a slope of 0° and (B) at a slope of 25° slope. A, Kruskal-Wallis by ranks analysis was performed for Vpeak. †p<0.05, indicates a significant difference vs. the 6-mo group of the same genotype, and $p<0.05 indicates a significant difference vs. the 9-mo group of the same genotype. Vpeak at 0°, Number of the test (NT) at 6mo=31, NT at 9-mo control = 20, NT at 18-mo control =11; NT at 6-mo Mt-CK$^{-/-}$ =38, NT 9-mo Mt-CK$^{-/-}$ =26, NT 18-mo Mt-CK$^{-/-}$ =10.

Vpeak at 25°, Number of the test (NT) at 6mo=24 NT at 9-mo control = 13, NT at 18-mo control =11; NT at 6-mo Mt-CK$^{-/-}$ =10, NT 9-mo Mt-CK$^{-/-}$ =18, NT 18-mo Mt-CK$^{-/-}$ =9.

Figure 4. Assay of the blood lactate level 5 min after the end of the incremental test (A) at a slope of 0° slope, (B) At a slope of *25°*. In a *post hoc* test, *p<0.05 and **p<0.01 indicate a significant difference vs. controls of the same age, ††p<0.01 and †††p<0.001 indicate a significant difference vs. the 6-mo group of the same genotype and $p<0.05, indicates a significant difference vs. the 9-mo group of the same genotype . 6-mo control n=12, 9-mo control n=10, 18-mo control n=10; 6-mo Mt-CK$^{-/-}$ n=13, 9-mo Mt-CK$^{-/-}$ n=13, 18-mo Mt-CK$^{-/-}$ n=8

Figure 5. (A) The score plot from the OPLS model were obtained for urine samples collected in the control group (blue dots, n=7; at 6-mo) and the Mt-CK$^{-/-}$ group (red dots, n=8; at 6-mo). Each score plot is given with its Q^2_Y and R^2_Y values (B) Heatmap of the correlation coefficients between metabolites and group classification. Only metabolites with R > 0.5 are represented (discriminant metabolites); trimethylamine N-oxide (TMAO), trimethylamine (TMA), Dimethylamine (DMA); 6-mo control n=7, 6-mo Mt-CK$^{-/-}$ n=8.

Figure 6. Protein expression in the quadriceps: (A) PGC-1α. (B) Mnf2. (C) OPA-1. (D) Drp-1. In a *post hoc* test, ††p<0.01 indicates a significant difference vs. the 6-mo group of the same genotype, and $p<0.05 indicates a significant difference vs. the 9-mo group of the same genotype . 6-mo control n=9, 9-mo control n=7, 18-mo control n=6, 6-mo Mt-CK$^{-/-}$ n=8, 9-mo Mt-CK$^{-/-}$, n=7, 18-mo Mt-CK$^{-/-}$ n= 6.

Figure 1.

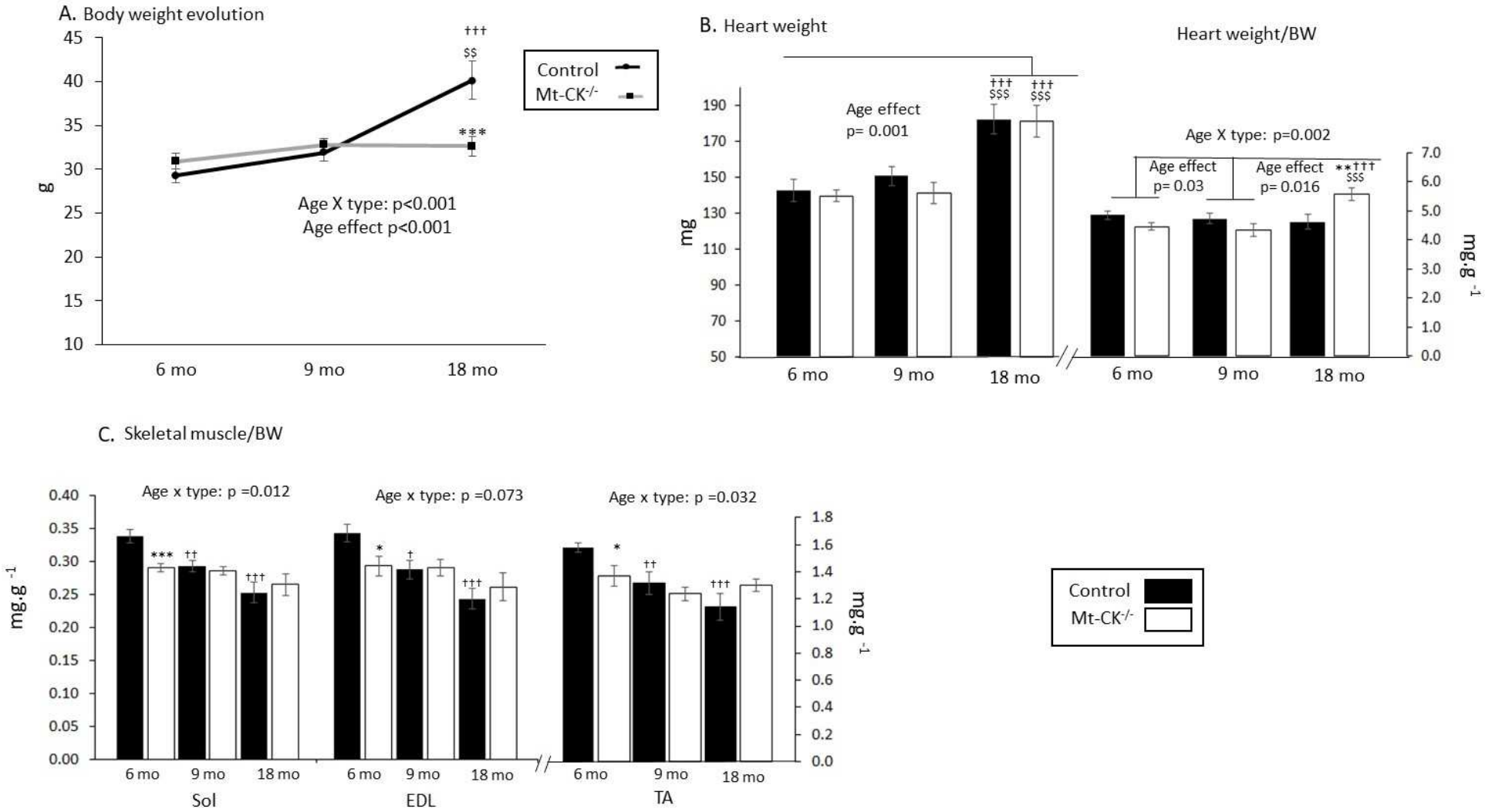
A. Body weight evolution
g
Control
Mt-CK-/-
Age X type: p<0.001
Age effect p<0.001
6 mo
9 mo
18 mo
B. Heart weight
Heart weight/BW
mg
mg.g-1
Age effect
p= 0.001
Age X type: p=0.002
Age effect
p= 0.03
Age effect
p= 0.016
C. Skeletal muscle/BW
mg.g-1
Age x type: p =0.012
Age x type: p =0.073
Age x type: p =0.032
Sol
EDL
TA
Control
Mt-CK-/-

Figure 2

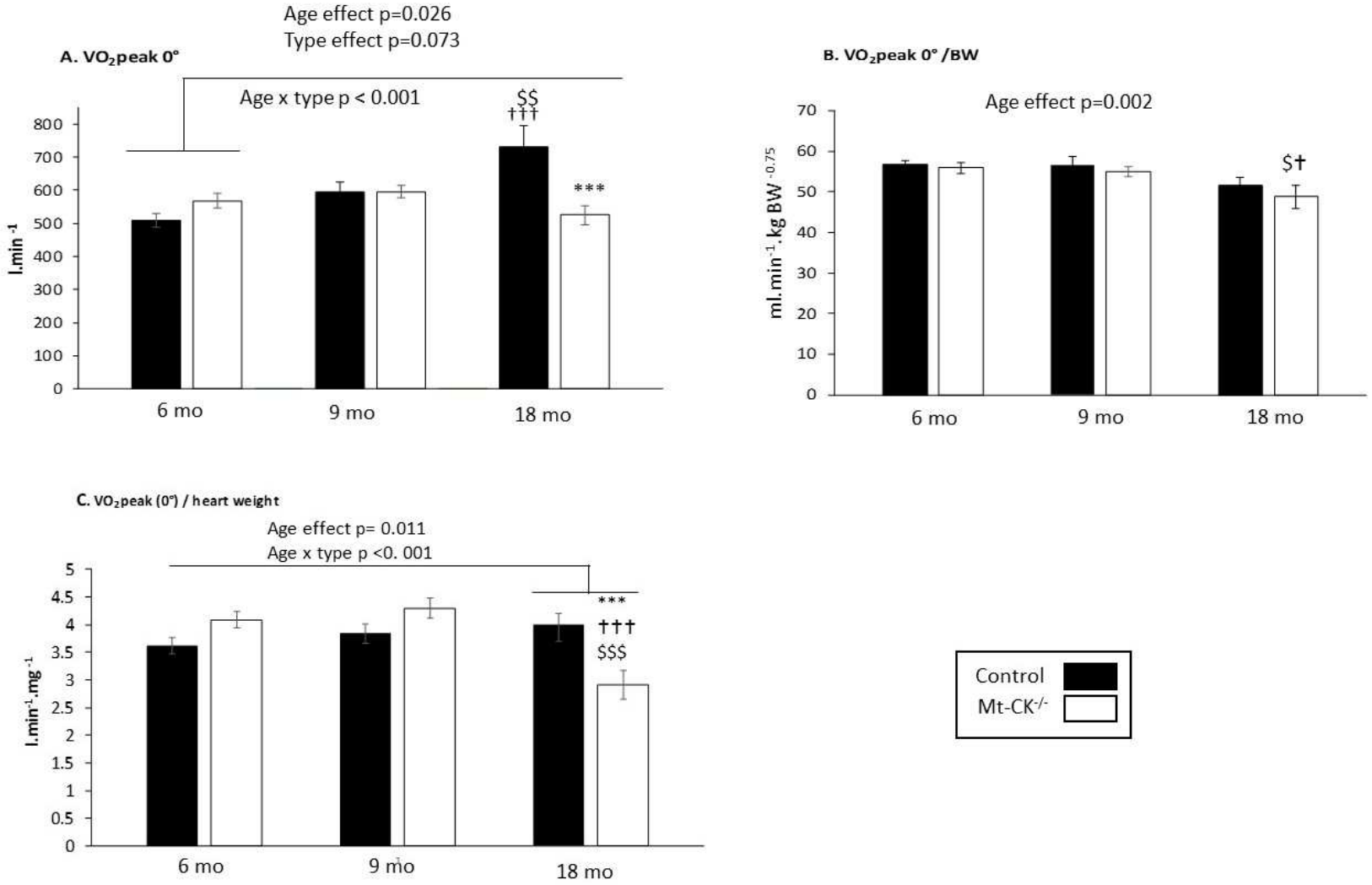
Age effect p=0.026
Type effect p=0.073
A. VO2peak 0°
Age x type p < 0.001
$$
†††
***
l.min -1
800
700
600
500
400
300
200
100
0
6 mo
9 mo
18 mo
B. VO2peak 0° /BW
Age effect p=0.002
$†
ml.min-1.kg BW -0.75
70
60
50
40
30
20
10
0
6 mo
9 mo
18 mo
C. VO2peak (0°) / heart weight
Age effect p= 0.011
Age x type p <0. 001
***
†††
$$$
l.min-1.mg-1
5
4.5
4
3.5
3
2.5
2
1.5
1
0.5
0
6 mo
9 mo
18 mo
Control
Mt-CK-/-

Figure 3.

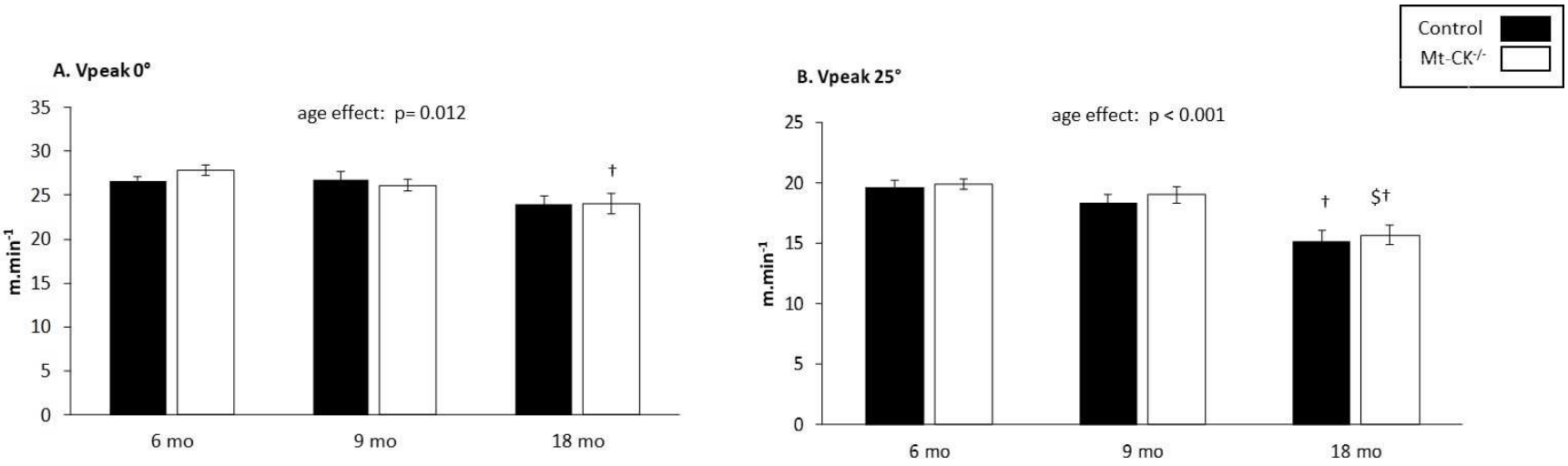
A. Vpeak 0°
age effect: p= 0.012
m.min-1
35
30
25
20
15
10
5
0
†
6 mo
9 mo
18 mo
B. Vpeak 25°
age effect: p < 0.001
m.min-1
25
20
15
10
5
0
†
$†
6 mo
9 mo
18 mo
Control
Mt-CK-/-

Figure 4.

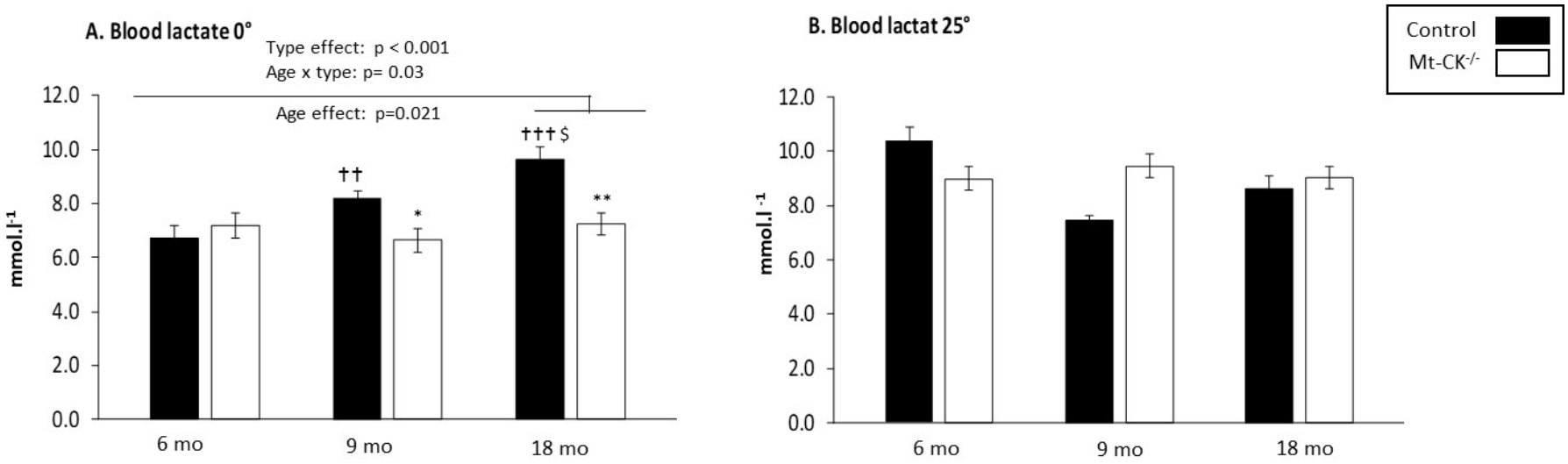
A. Blood lactate 0°
Type effect: p < 0.001
Age x type: p= 0.03
Age effect: p=0.021
mmol.l-1
12.0
10.0
8.0
6.0
4.0
2.0
0.0
6 mo
9 mo
18 mo
††
†††$
*
**
B. Blood lactat 25°
Control
Mt-CK-/-

Figure 5.

A.

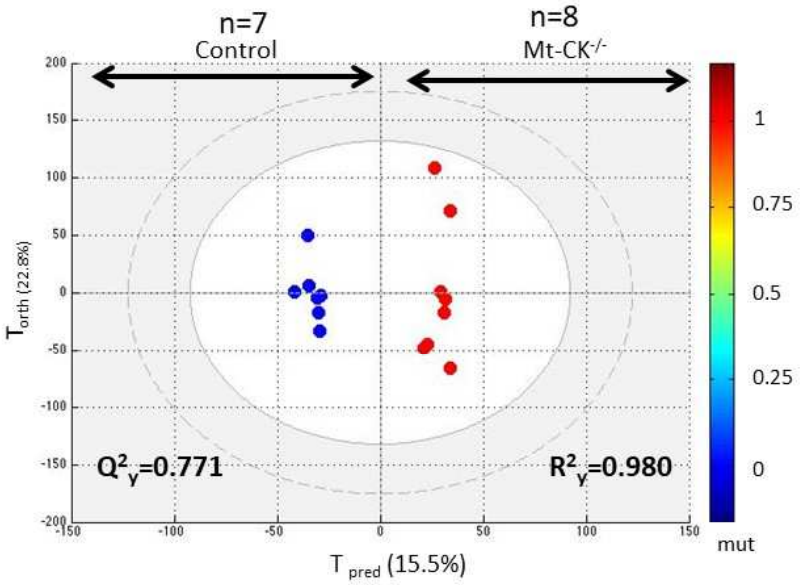
n=7
Control
n=8
Mt-CK-/-
Q2Y=0.771
R2Y=0.980
Torth (22.8%)
T pred (15.5%)
1
0.75
0.5
0.25
0
mut

B.

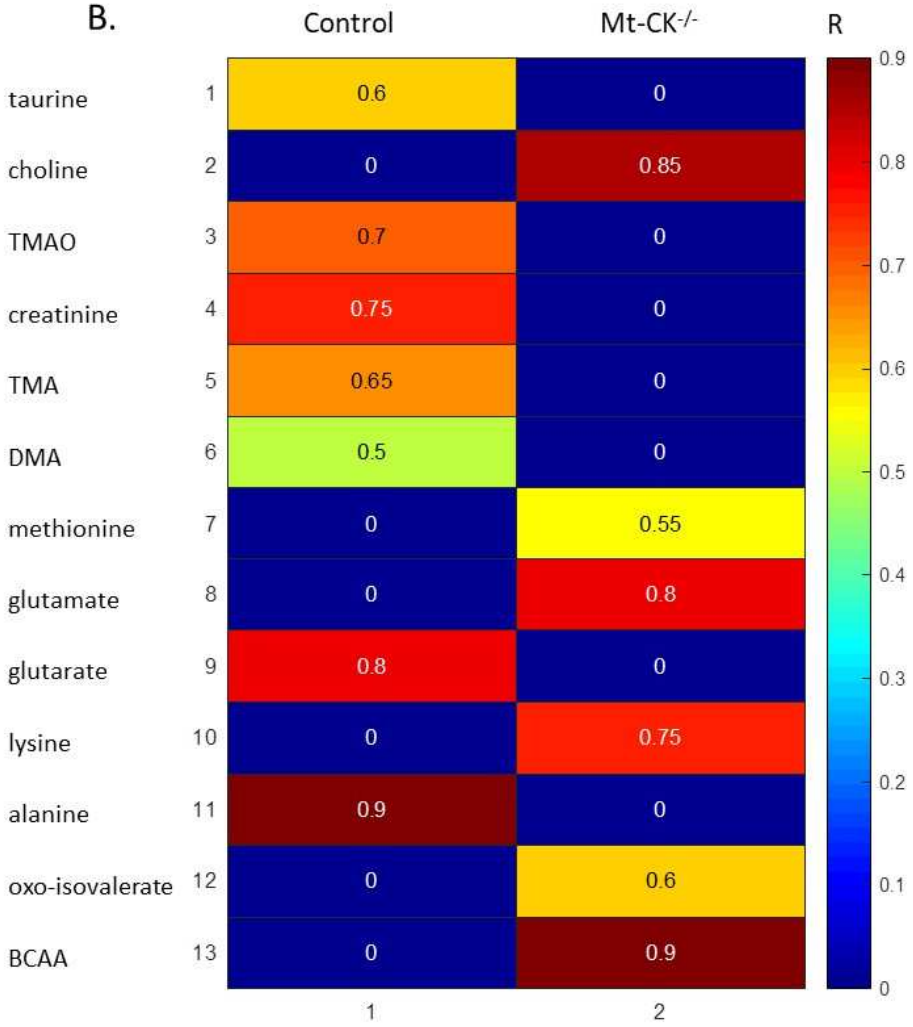
Control
Mt-CK-/-
R
taurine 1 0.6 0
choline 2 0 0.85
TMAO 3 0.7 0
creatinine 4 0.75 0
TMA 5 0.65 0
DMA 6 0.5 0
methionine 7 0 0.55
glutamate 8 0 0.8
glutarate 9 0.8 0
lysine 10 0 0.75
alanine 11 0.9 0
oxo-isovalerate 12 0 0.6
BCAA 13 0 0.9
1
2
0.9
0.8
0.7
0.6
0.5
0.4
0.3
0.2
0.1
0

Figure 6.

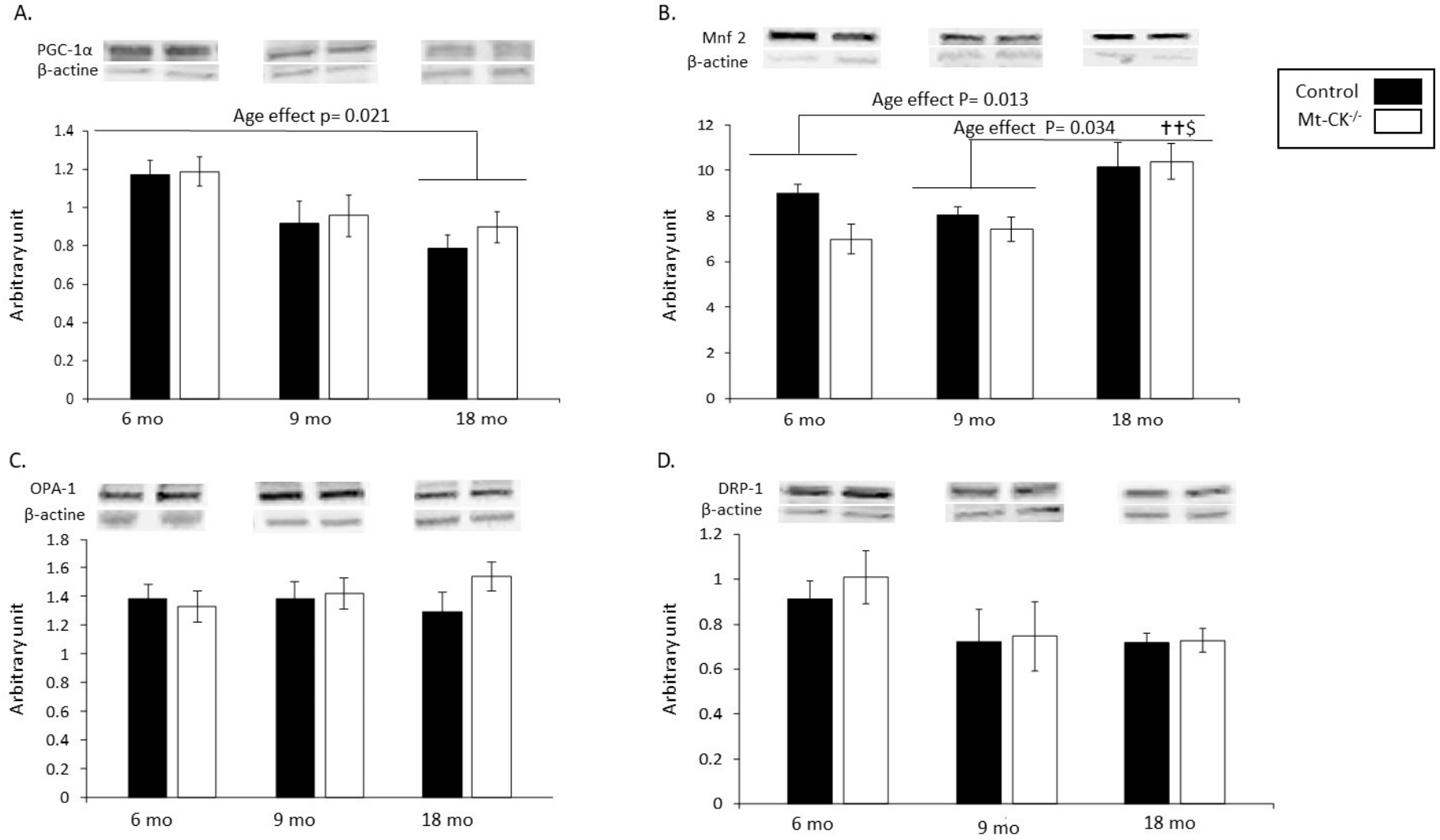
A.
PGC-1α
β-actine
Age effect p= 0.021
Arbitrary unit
1.4
1.2
1
0.8
0.6
0.4
0.2
0
6 mo
9 mo
18 mo
B.
Mnf 2
β-actine
Age effect P= 0.013
Age effect P= 0.034
††$
Arbitrary unit
12
10
8
6
4
2
0
6 mo
9 mo
18 mo
Control
Mt-CK-/-
C.
OPA-1
β-actine
Arbitrary unit
1.8
1.6
1.4
1.2
1
0.8
0.6
0.4
0.2
0
6 mo
9 mo
18 mo
D.
DRP-1
β-actine
Arbitrary unit
1.2
1
0.8
0.6
0.4
0.2
0
6 mo
9 mo
18 mo